Final Report

submitted to

NATIONAL AERONAUTICS AND SPACE ADMINISTRATION
GEORGE C. MARSHALL SPACE FLIGHT CENTER, ALABAMA 35812

August 24, 1992

for Contract NAS8 - 36955

Delivery Order 135

entitled

# Study of Eddy Current Probes

by

Gary L. Workman Ph.D.
Principal Investigator
and
Morgan Wang
Graduate Student

Materials Processing Laboratory
Center for Automation & Robotics
University of Alabama in Huntsville
Huntsville, Alabama 35899

# Report Documentation Page

| 1. Report No. | 2. Government Accession No. | 3. Recipient's Catalog No. |
|---|---|---|
| | | |

**4. Title and Subtitle**

"Eddy Current Probes"

**5. Report Date**

**6. Performing Organization Code**

UAH/JRC

**7. Author(s)**

Gary L. Workman

**8. Performing Organization Report No.**

**10. Work Unit No.**

**9. Performing Organization Name and Address**

University of Alabama in Huntsville
Research Institute Box 212
Huntsville, AL 35899

**11. Contract or Grant No.**

NAS8-36955

**13. Type of Report and Period Covered**

~~Monthly~~ Final

**12. Sponsoring Agency Name and Address**

Marshall Space Flight Center

**14. Sponsoring Agency Code**

NASA/MSFC

**15. Supplementary Notes**

**16. Abstract**

The recognition of defects in materials properties still presents a number of problems for nondestructive testing in aerospace systems. This project attempts to utilize current capabilities in eddy current instrumentation, artificial intelligence and robotics in order to provide insight into defining geometrical aspects of flaws in composite materials which are capable of being evaluated using eddy current inspection techniques.

**17. Key Words (Suggested by Author(s))**

Nondestructive Evaluation, Expert Systems
Defect Recognition, Eddy Current Testing
Composites

**18. Distribution Statement**

cc:
CN-22D (3)
AT-01 (1)
CN-01/Wofford (1)
EM-13/L. Smith (1)
ONRRR (1)
ES-52/J.M. Davis (2 + repro)
NASA/Sci & Tech Info. Fac. (1 + repro)
Vaughan/UAH (1)

| 19. Security Classif. (of this report) | 20. Security Classif. (of this page) | 21. No. of pages | 22. Price |
|---|---|---|---|
| | | | |

TABLE OF CONTENTS

## INTRODUCTION

Eddy current inspection of graphite epoxy filament wound materials has been investigated by several researchers[1-12]. The results of these investigations show considerable promise for eddy current testing to locate flaws such as cut tows and impact damage in critical structures fabricated from graphite filaments. Detection of delaminations in such materials is more difficult in that voids in the conducting media, such as observed in kissing debonds, do not always exist naturally. Loaded samples may be more easily inspected however, because of possible displacement of the laminae surfaces to create a non-conducting volume that is observable using eddy currents.

Earlier work of this research group resulted in the developement of a robotic scanning eddy current inspection cell which is located in Building 4702 at Marshall Space Flight Center. A MacIntosh FX computer with a Symbolics McIvory board set provided the computational and control function. However, eddy current sensing was performed with either a Smarteddy (PC platform) or a HP 4193A Impedance Meter. Data conversions to get the data into the MacIntosh were either cumbersome in the former case or extremely slow in the latter case. Consequently this work concentrated on designing and building an eddy current interface for the MacIvory which could replace both of the above instruments for acquiring eddy current signals.

The basic concept for this research activity is presented in Figure 1. Manual inspection, particularly for either large filament wound items or large volumes of small cylindrical items, would be a very inefficient and tedious process. Eddy current waveforms of the composite filament componentsare rather noisy since the filaments themselves provide a time varying signal as the probe scans over them. Any other motions caused by manual scanning manipulations would then add to the already modulated signal normally expected and would make interpretation more difficult. Consequently this research has concentrated on automated systems approach. Adding an expert system to the interpretation is still a major goal once a correct set of interpretation procedures have been accomplished.

Figure 1. Overall Systems Concept for the Robotic Eddy Current Inspection Workcell.

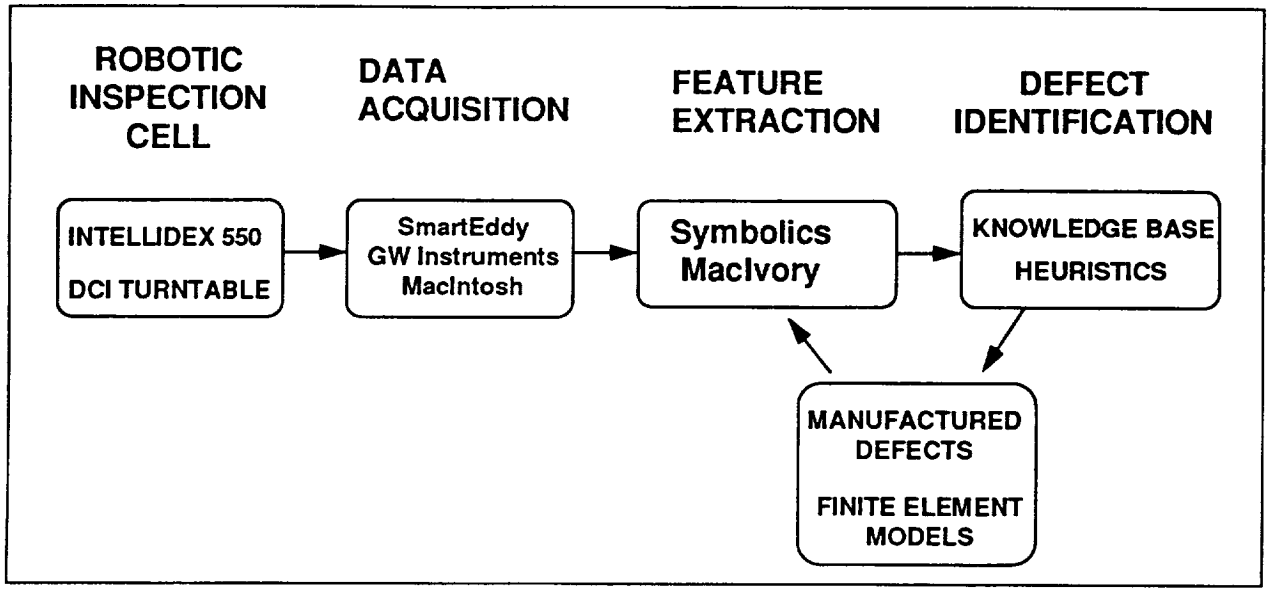


## EXPERIMENTAL

### Workcell Components

The Robotic Scanning Laboratory at the NDE Laboratory at MSFC consists of the workcell items as shown in Figure 1. An Indellidex 550 robot is used to orient various eddy current probes onto the part under test and perform scaning operations. The five degrees of freedom available in the robot arm are augmented by a DCI turntable which rotates the item under test. All control functions are programmed through the MacIntosh system running Labview. A sketch showing how the eddy current transducer atached to the robot end-effector approaches the item under test is shown in Figure 2. Due to the flexibility of the robotic end-effector a variety of probes and trajectories are available for NDE applications.

Figure 2. Position of Robot Arm in Approaching Part Under Test

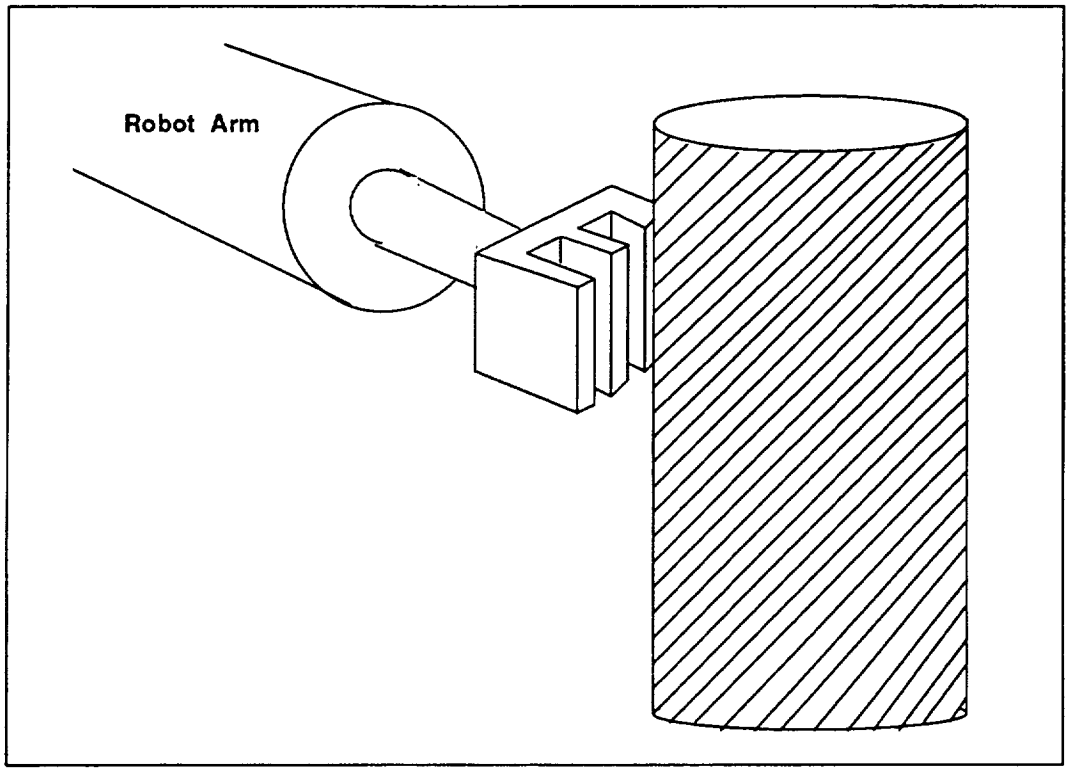


Notice that the transducer shown in Figure 2 is an E-probe. As part of this work, we have fabricated several types of probe assemblies to be used with the robot system, including a horseshoe, an E-probe, a cup probe and a pancake probe. the dimensions of these probes are shown in Figure 3. Each probe uses ferrite material to concentrate the magnetic flux into the part under test. The ferrite material for all probes except the pancake probe was a high permeability ferrite component from Magnetics, Inc. The ferrite rod used to prepare the pancake probe was obtained through a local electronics parts supplier.

Figure 3. Various Eddy Current Probes Used to Inspect Graphite Epoxy Components

E-Probe

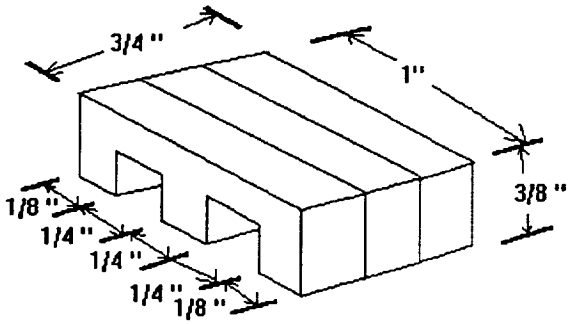


Cup Probe

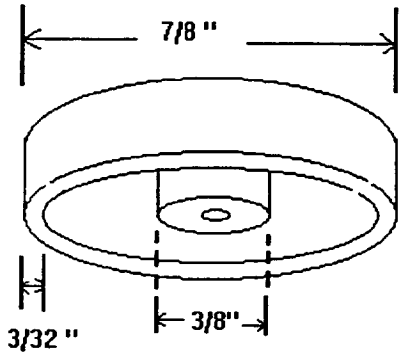


Horseshoe Probe

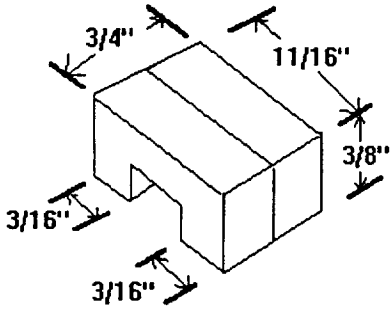


Pancake Probe

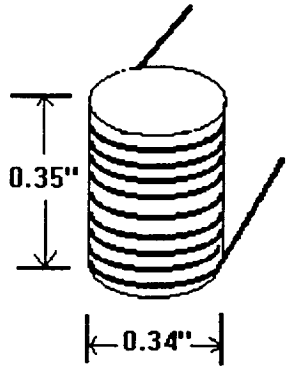


Eddy Current Instrumentation Concepts

The earlier work used the HP 4193A to generate and acquire the eddy current signals for the graphite epoxy samples. Since the maximum data sampling rate was very slow (7 readings per second), a major effort was made to develop the capability for faster data sampling in a mode that was compatible with the MacIntosh computer system. In order to accomplish this task, we chose to fabricate our own circuitry for acquiring the eddy current signals and thus to use the HP 4193 only to generate the

alternating current needed to generate eddy currents. Figure 4 shows the instrumental concept employed for both both generating, decoding phase and magnitude, and acquiring the eddy current signals.

Figure 4. Schematic of Eddy Current Source and Detection System Used in this Work.

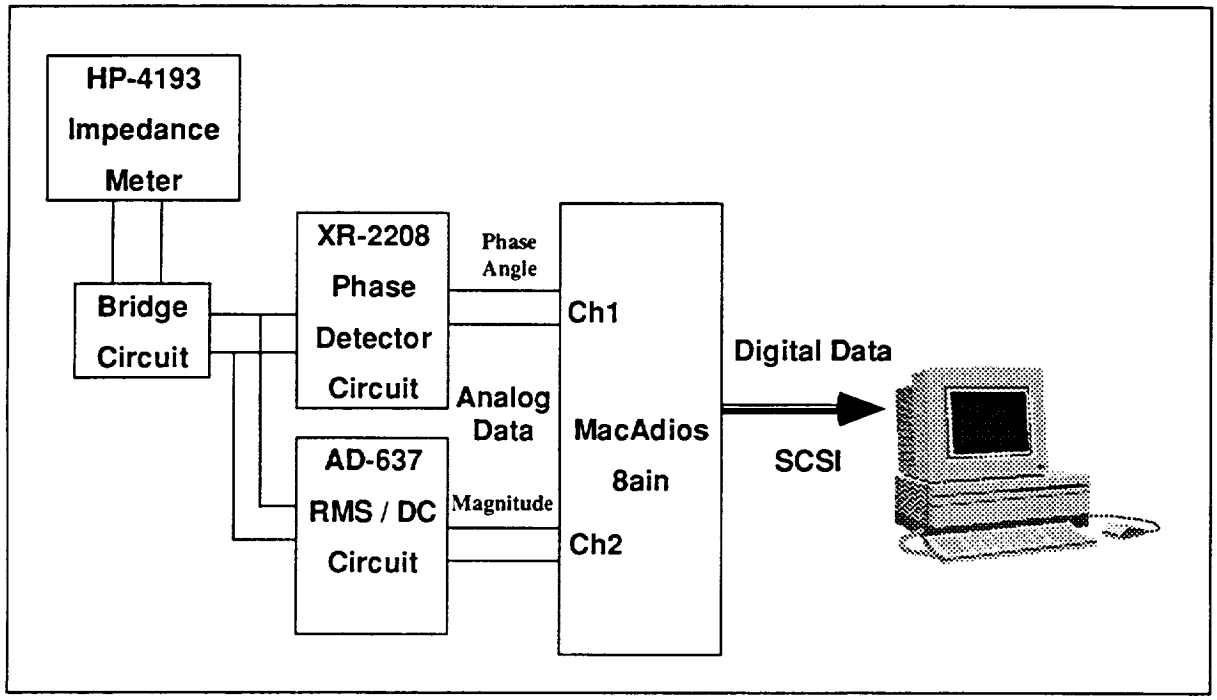


The circuitry used here is very similar to other systems and uses the XAR 2208 RMS-DC converter devices to generate a dc level signal from the ac signals observed during the eddy current scan. Using two XR 2208's allows both the phase and the magnitude to be digitized and acquired with a GW Instruments A/D converter. The GW Instruments A/D uses the SCSI bus to transfer the digitized data to the MacIntosh.

Figure 5. Schematic of Bridge Circuit used to acquire Eddy Current Signals.

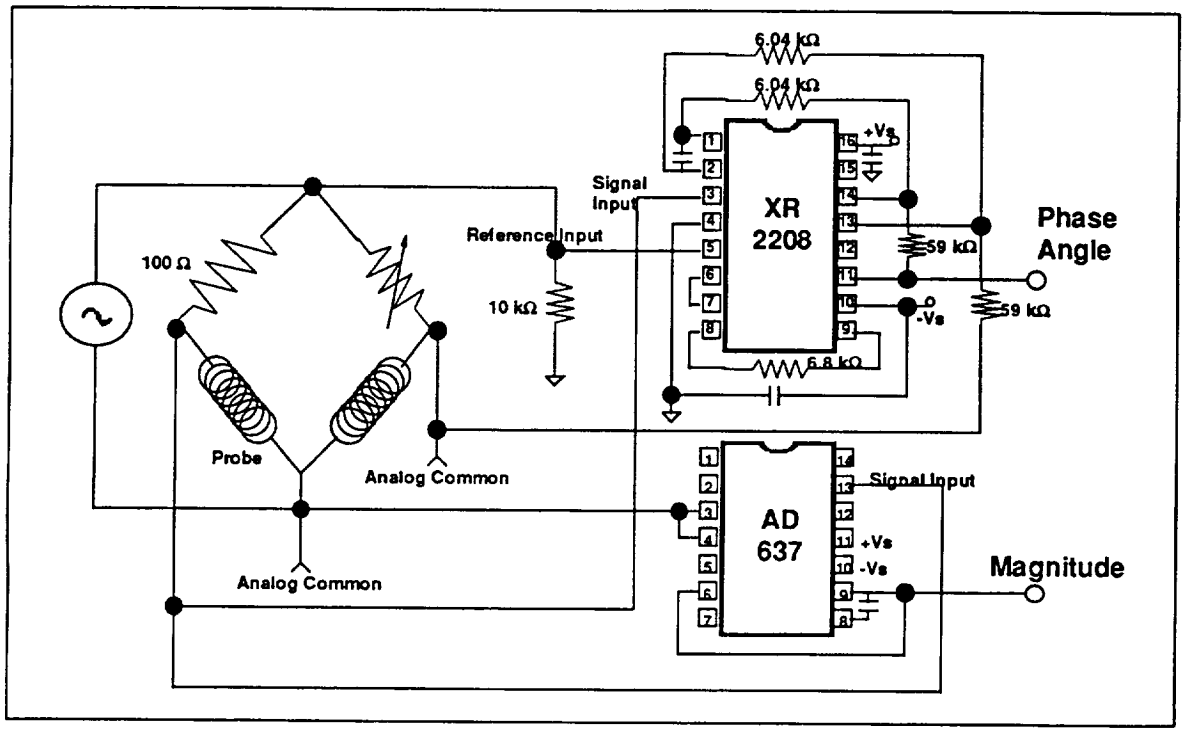


Test Specimens

Cylindrical samples of graphite epoxy with two different thicknesses were used for these studies. These samples were prepared by MSFC personnel in their filament winding laboratory in Building 4707. The first specimen was a four ply, 12 inch in diameter cylinder, representative of thin specimens. The second specimen was 24 plies thick with the same diameter. The layout of the manufactured defects for the two specimens are shown in Figures 6 and 7 on the next page. The depth of penetration for these specimens is shown in Figure 8. This plot allows one to determine sensitivity for flaw detection according to ply number in the composite.

Figure 6. Manufactured defects for four ply test cylinder.

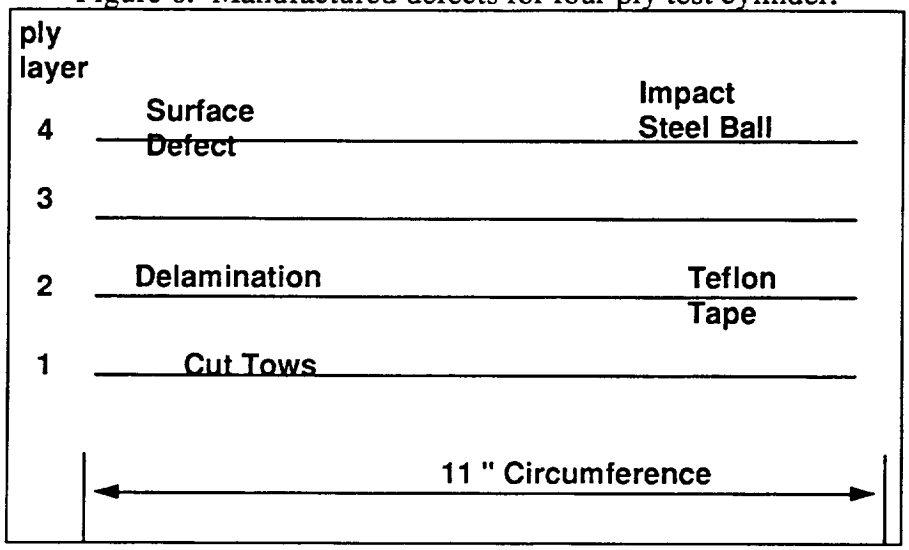


Figure 7. Manufactured Defects for Thick specimen

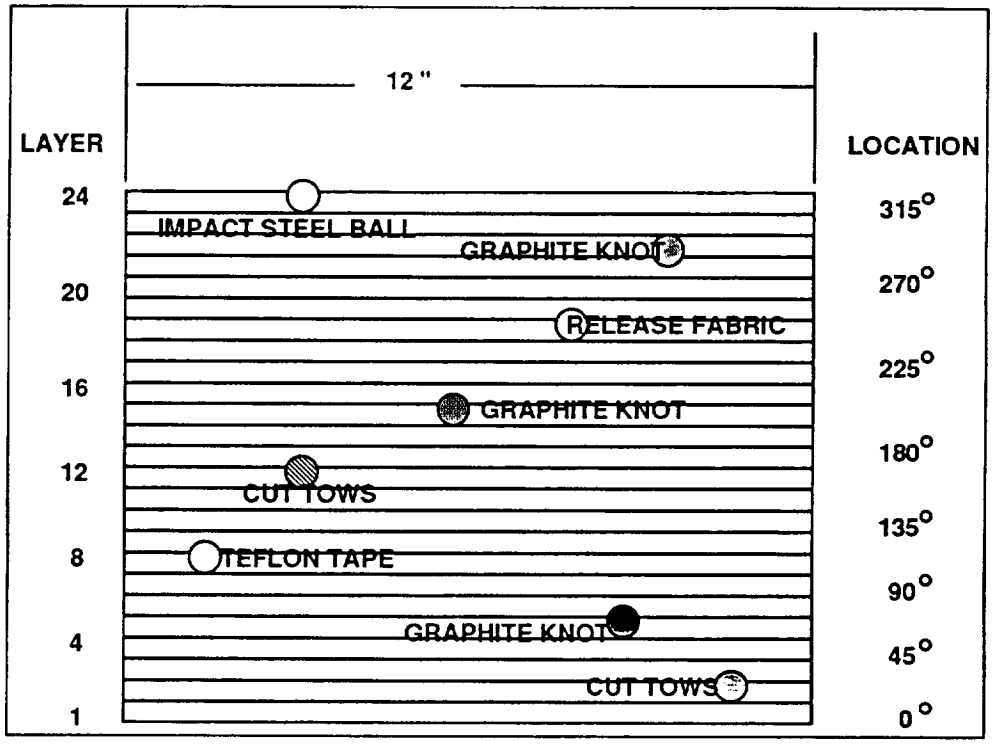

Figure 8. Depth of Penetration of Graphite Epoxy at 3.2 Mhz

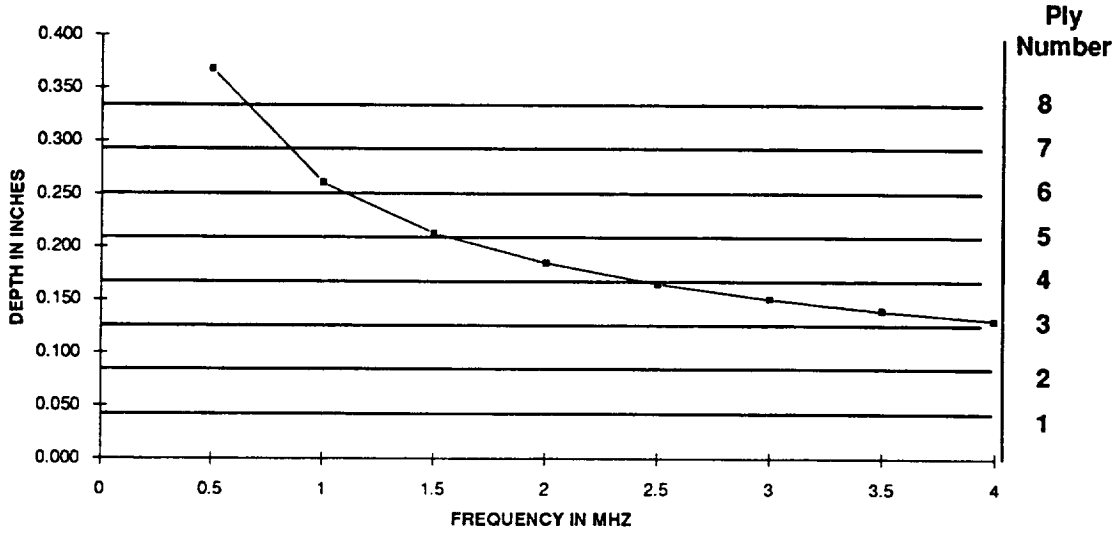


Quantitative Modeling Of Responses In Eddy Current Probes

The ability to characterize unknown defects detected by the eddy current method is limited by the lack of adequate theoretical models. Basically, such models should take the place of very difficult and expensive experiments in developing the knowledge base necessary to approach the inverse problem that given a particular eddy current response, characterize the defect. Extensive developments of the finite element method for eddy current problems has been very successful for two-dimensional or axisymmetric geometries. However, the difficulties occur in the FEM three-dimensional case due to the large number of nodes required and the necessity for three non-zero components of the magnetic vector potential.

The FEM model should be most efficient for rather large-size defects because the number of nodes necessary to map the fields adequately is then relatively small. The model developed by Burrows[33] gives the response to defects of spheroidal shape with dimensions small compared with the skin depth in the materials. The boundary-element integral equation model of Hower[34] has allowed consideration of defects of various shapes but with the same size restriction. Still needed is an efficient method for calculating the effect of three-dimensional defects having dimensions up to one to two skin depths.

The model developed in this work can be considered as a hybrid approach utilizing several available techniques. The method involves separation of the problem into three parts: (1) Use a commercially available finite element software, Ansoft Maxwell in our case, to calculate the incident fields of the horseshoe probe, but in the absence of any defect. (2) Compute the total fields on the surface of the defect. (3) Determine the resulting change in probe coil impedance from both unperturbed fields

and equivalent source on the defect surface using the Lorentz reciprocity theorem. The mathematical foundation for this operation follows below.

The change in coil impedance $\Delta Z$ due to the flaw can be found in terms of an integral of the field quantities E and $E_0$ (the fields at the position of flaw with and without the flaw being present). These formulas have been derived by Auld[29] and Zaman, et al[30].

Let us assume that within a linear, isotropic medium, which is not necessarily homogeneous, there exist two sets of sources $J_1$, $M_1$ that are allowed to radiate simultaneously or individually inside the same medium at the same frequency and produce fields $E_1$, $H_1$ and $E_2$, $H_2$ respectively. The field equations are then:

$$\nabla \times H_1 = J_1 + j\omega\varepsilon E_1 \quad (1)$$
$$\nabla \times E_1 = -M_1 + j\omega\varepsilon H_1 \quad (2)$$
$$\nabla \times H_2 = J_2 + j\omega\varepsilon E_2 \quad (3)$$
$$\nabla \times E_2 = -M_1 + j\omega\varepsilon H_2 \quad (4)$$

We multiply Equation (1) scalarly by $E_2$ and equation (4) by $H_1$ and add the resulting equations. Similarly Equations (2) and (3) to give:

$$\nabla ( E_2 \times H_1) = + j\omega\varepsilon E_1 E_2 + j\omega\varepsilon H_1 H_2 + E_2 J_1 + H_1 M_2$$
$$\nabla ( E_1 \times H_2) = + j\omega\varepsilon E_1 E_2 + j\omega\varepsilon H_1 H_2 + E_1 J_2 + H_2 M_1$$

where the left-hand term has been simplified by the vector identities. A subtraction of the former equation from the latter yields:

$$\nabla ( E_1 \times H_2 - E_2 \times H_1 ) = E_2 J_1 - E_1 J_2 + H_1 M_2 - H_2 M_1$$

At any point for which the fields are source-free (J=M=0) this reduces to:

$$\nabla ( E_1 \times H_2 - E_2 \times H_1 ) = 0$$

which is called the special case of Lorentz reciprocity theorem. Its integral form is:

$$\int_s ( E_1 \times H_2 - E_2 \times H_1 ) \, dS \quad (5)$$

Expression for the change in coil impedance ($\Delta Z$) are obtained by application of above reciprocity theorem.

The simplest geometry appropriate to this problem is the case shown in Figure 9. It consists of a conductive body B, a defect and a eddy current horseshoe probe. Identify the multiply connected region bounded by the surface $S_d$ of the defect, the closed surface $S_S$ surrounding the source, the cable cross-section $S_C$ and a boundary at infinity $S_\infty$. Let the volume enclosed by this surface be V and $E_0$, $H_0$ denote the time harmonic fields

when the defect dose not exist and E, H denote the field actually existing with the defect present.

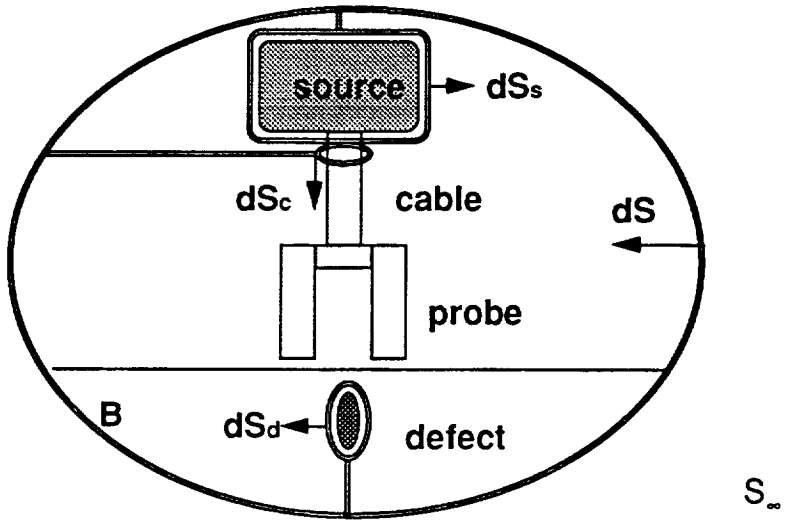


Figure 9 Geometry of eddy current problems.

Since the volume V contains no source currents (the scattered fields are considered as being due to surface currents on $S_d$) and the material within V is identical with or without the presence of defect, the Lorentz reciprocity theorem is valid,

$$\int_S ( E_0 \times H - E \times H_0 ) \, dS = 0$$

where dS is an element of surface which is normal to and directed into the bounded volume. The surface S is the sum of surfaces which include $S_\infty$, $S_c$, $S_S$ and $S_d$. However,

$$\int_S = \int_\infty + \int_{S_c} + \int_{S_s} + \int_{S_d} = 0$$

Since the integrand goes to zero on $S_\infty$, as this partial surface is allowed to move to infinity, and it also goes to zero on the source enclosure $S_S$, if it is assumed to be perfectly conducting. There remains the feed line cross-section $S_c$ and the surface $S_d$ enclosing the defect. Hence, we have

$$\int_{S_c} ( E_0 \times H - E \times H_0 ) \, dS = \int_{S_d} ( E_0 \times H - E \times H_0 ) \, dS \qquad (6)$$

Assuming a coaxial cable feed line, the surface $S_c$ appears as shown in Figure 10. If the field quantities in Equation 5 are defined as those produced (either in the absence or the presence of the defect) by a drive current $I$ at the surface $S_c$, then the magnetic fields on $S_c$ are

$$H_\varphi = H_{0\varphi} = \frac{1}{2\pi r}$$

in terms of the feed line current $I$; and the feed line voltages in the absence and presence of the flaw are given in terms of the electric fields by

$$\int E_r dr = -ZI, \int E_{0r}\, dr = -Z_0$$

where $Z$ designates the circuit impedances at this point in the line. Note that the field distributions, which are those characteristic of a coaxial line, are unchanged by the presence of the defect because of the way these fields are normalized, only the electric field is changed in magnitude. From this, it is found

$$\int_{S_c} (E_0 \times H - E \times H_0)\, dS = \int_{S_d} (E_0 \times H_\varphi - E_r \times H_{0\varphi})\, dS = I^2 (Z0 - Z) \qquad (7)$$

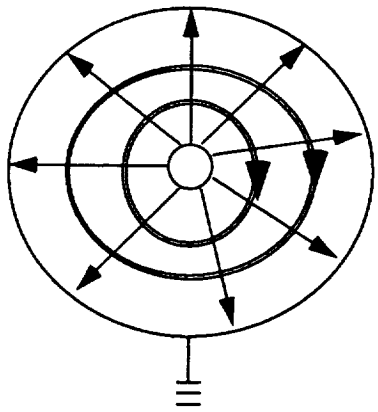


Figure 10. Distribution of electrical and magnetic fields inside a coaxial transmission line.

Substitute Equation (7) into Equation (6), gives

$$I^2 (Z0 - Z) = - \int_{S_d} ( E_0 \times H - E \times H_0 ) \, dS \qquad (8)$$

$$\therefore \qquad \Delta Z = (Z_0 - Z) = -\frac{1}{I^2} \int_{S_d} ( E_0 \times H - E \times H_0 ) \, dS \qquad (9)$$

Using Gauss's theorem,

$$\Delta Z = -\frac{1}{I^2} \int_{V_d} [H \cdot (\nabla \cdot \times E_0) - E_0 \cdot (\nabla \times H) - H_0 \ (\nabla \cdot \times E) + E \cdot (\nabla \cdot \times H_0 )] \, dV$$

$$\Delta Z = -\frac{1}{I^2} \int_{V_d} [H \cdot (-j\omega\mu_0) - E_0 \cdot (j\omega\varepsilon E) - H_0 \ (-j\omega\mu_0 H) + E \cdot (j\omega\varepsilon E_0)] dV$$

$$\Delta Z = \frac{j\omega(\varepsilon - \varepsilon_0)}{I^2} \int_{V_d} E_0 \bullet E dV$$

But

$$\varepsilon = \varepsilon_0 - \frac{j\sigma}{\omega}, \quad \therefore \varepsilon - \varepsilon_0 = -\frac{j\sigma}{\omega}$$

$$\Delta Z = \frac{\sigma}{I^2} \int_{V_d} E_0 \bullet E dV \qquad (10)$$

where E and $E_0$ are the electric fields with and without the defect present. Equation (10) is the formula that we use in this work.

The case of a defect whose permittivity is near that of the host material may be examined in greater detail by allowing the field in the presence of the defect E to be approximated by the unperturbed field $E_0$ over the volume of the defect. For defects small enough that the fields do not vary greatly over its volume, the expression may be further approximated by using just the value of the field at the position of the centroid of the defect,

$$\Delta Z = \frac{\sigma V_d}{I^2} E_0^2 \qquad (11)$$

Similar derivations for the change in impedance due to a flaw have also been developed by Bahr[31] and by Auld [32]. The expression derived here in Equation (11)

corresponds to a low frequency approximation, and the fields are already known for the unflawed case. It can provide a simpler first order approximation for the change in complex impedance. The approximation that $E = E_0$ is more accurate for case in which the e and s of the defect differ only slightly from that of host material. In this research work, the FEM model can calculate both the E and $E_0$, so Equation (10) is used to solve for $\Delta Z$.

Traditionally, eddy current nondestructive evaluation methods have been used only to provide qualitative information regarding the presence or absence of a defect. However, the measured data also contain quantitative information about the defect size. From the finite element method and electromagnetic reciprocity relation, the impedance change at the probe terminals is formulated in terms of an electromagnetic field integral over a surface surrounding the defect. In this section the two-dimensional finite element model of E and horseshoe probe on the single layer isotropic material and also the calculation of the fields inside the materials is presented.

Figure 11 shows the horseshoe probe as it passes over a defect. Although the two-dimensional case is not a realistic model of any actual defect configuration, it does serve to bring out the general nature of the probe-defect interaction problems.

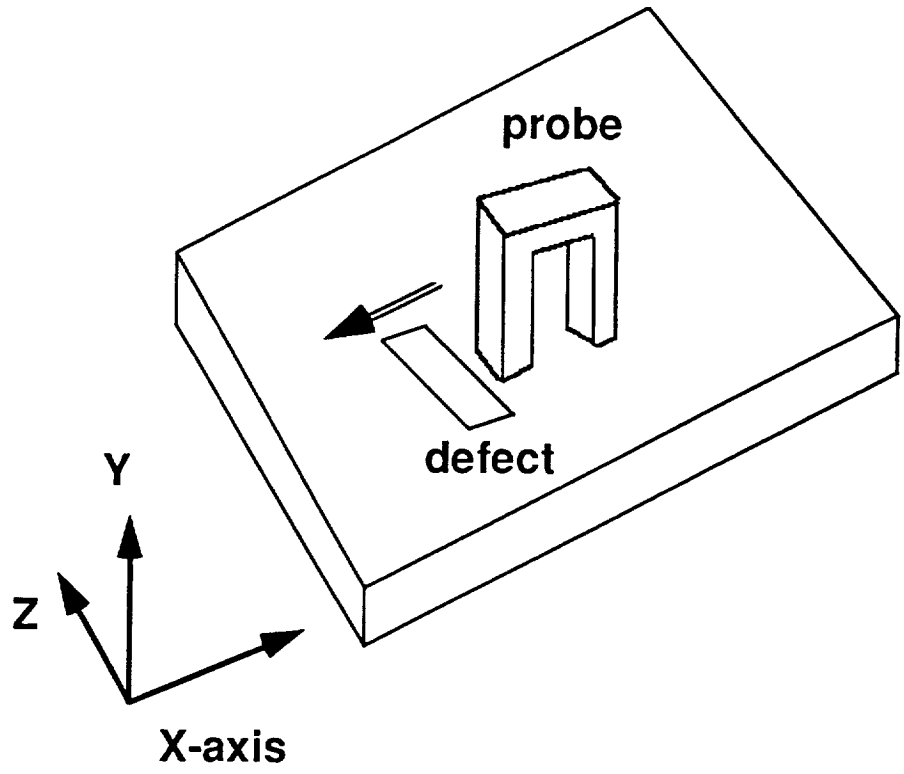


Figure 11 Eddy current horseshoe probe scan through the specimen with a defect.

The defect response is calculated from the value of the magnetic vector potential,

$$Z = \frac{j\omega}{I_s} \oint A dt$$

where $I_S$ is the source current. Because the magnetic vector potential has only one component in the direction of the current for one turn of a coil have a radius r, the impedance is:

$$Z_i = \frac{j\omega 2\pi r_i A_i}{I_s}$$

where $A_i$ is the magnetic vector potential at $r_i$. Integrating Equation (12) over an elemental area with $N_S$ turns per unit area the expression becomes:

$$Z_i = \frac{j\omega 2\pi r_{ci} A_{ci} N_s \Delta_i}{I_s}$$

where $r_{ci}$ is the distance from axis to the centroid of the element, $A_{ci}$ is the magnetic vector potential at the centroid of the element and $D_i$ is the area of the element respectively. Summing Equation (13) over the elements in the coil's cross section and noting that $J_S=N_SI_S$, the coil impedance is:

$$Z_{coil} = \frac{j\omega 2\pi J_s}{I_s^2} \sum_{i=1}^{N} r_{ci} \Delta_i A_{ci} \qquad (14)$$

In three-dimensional geometries, this method can not be used because it assumes that the magnetic vector potential is constant along the circumference of the coil. However, the Lorentz reciprocity theorem allows us to calculate the three-dimensional defect response of the horseshoe probe (uniform field probe).

Electromagnetic fields in a uniaxial conductor have been studied in order to evaluate the eddy current testing of composite material such as graphite epoxy. It is important to understand how eddy currents behave in anisotropic material, especially uniaxial conductors (graphite fibers) in which the conductivity in the axial direction may be several hundred times greater than the transverse conductivity. Ansoft Maxwell Solver can model the anisotropic material if we set up the material parameters as a tensor or a function of position and frequency. But in this research work, all the parameters of graphite epoxy are unknowns.

Theoretical models of eddy current cylindrical air core probe on graphite epoxy have been developed by Bowler[22] and Beissner[33]. These solutions are given in terms of half-space scalar potential and dyadic Green's functions. Following Bowler, the corresponding electric and magnetic fields are:

$$\vec{E}_n = j\omega\mu_n[\nabla\times\hat{y}_n\Psi_n^{'} + \nabla\times\nabla\times\hat{y}_n\Psi_n^{''} + (1-\frac{\sigma_n^t}{\sigma_n^l})\hat{y}_n\nabla_t^2\Psi_n^{''}]$$

$$\vec{H}_n = \nabla_t\frac{d\Psi_n^{'}}{dy_n} - \hat{y}_n\nabla_t^2\Psi_n^{'} + \frac{2j}{\delta_t^2}\nabla\times\hat{y}_n\Psi_n^{''}$$

where

$$\nabla_t = \hat{x}_n\frac{d}{dx_n} + \hat{z}\frac{d}{dz}$$

$Y_n^{'}$ is transverse electric (TE) potential, $Y_n^{''}$ is the transverse magnetic (TM) potential for layer n. The potentials satisfy the equations

$$\nabla^2\Psi_n^{'} + \frac{2j}{(\delta_n^t)^2}\Psi_n^{''} = 0$$

and

$$\left[\frac{\sigma_n^l}{\sigma_n^t}\frac{d^2}{dy_n^2} + \nabla_t^2\right]\Psi_n^{''} + \frac{2j}{(\delta_n^l)}\Psi_n^{''} = 0$$

where TE and TM skin depths are:

$$\delta_n^t = \sqrt{\frac{2}{\omega\mu_n\sigma_n^t}}$$

$$\delta_n^t = \sqrt{\frac{2}{\omega\mu_n\sigma_n^l}}$$

The standard approach to the calculation of the impedance of an eddy current probe is through Auld's[29] reciprocity integral. In the composite material, the integral involves certain vector products of the probe field in free space and the fields on the top (z=0) and bottom surface (z=-t) of the layered structure. when the TE and TM scalar potentials are introduced, the TM component does not contribute to the impedance

integral. Thus we need only the transmitted and reflected TE potential to calculate the probe impedance change. According to Beissner [40], the integral leads to

$$\Delta Z = -\frac{2j\omega}{\mu_0 I^2}\int \frac{\hat{z}\bullet\vec{k}\times\vec{a}\left(\vec{k},0\right)}{k^2}\left[R(\vec{k})\hat{z}\bullet\vec{k}\times\vec{a}\left(-\vec{k},0\right)-T\left(\vec{k}\right)\hat{z}\bullet\vec{k}\times\vec{a}_s\left(-\vec{k},-t\right)\right]d$$

where $a_S(k,z)$ is the Fourier transform of the vector potential, R and T are the reflection and transmission coefficients, which defined by

$$u_R\left(\vec{k},0\right)=R\left(\vec{k}\right)u_s\left(\vec{k},0\right)$$

$$u_T\left(\vec{k},0\right)=T\left(\vec{k}\right)u_s\left(\vec{k},0\right)$$

where

$$u_s\left(\vec{k},z\right)=\frac{j}{\mu_0 k^2}\hat{z}\bullet\vec{k}\times\vec{a}_s\left(\vec{k},z\right)$$

and $u_R(k,0)$ is the Fourier transform of the reflected TE potential at Z=0, $u_T(k,-t)$ is the transmitted field at the bottom of the specimen (z=-t).

This model is equally applicable to any material that can be treated as a multilayer anisotropic conductor. The calculation procedure of Equation (14) can be modified for the different shape probes in the feature work.

ANSOFT MODELS

During this phase of the eddy current reserach, more procedures for utilizing Ansoft Maxwell finite element software were developed. The following simulation was developed for a 4-ply graphite epoxy filament wound component using the following values:

Graphite conductivity - 14, 300 $ohms^{-1}m^{-1}$
Ferrite conductivity - 1 $ohms^{-1}m^{-1}$
Ferrite permeability - 2, 500
Ply thickness 0.052 inches
Ferrite dimensions - see chart below
Flaw dimension - 0.1 x 0.052 $inches^2$
Frequency - 3.2 megahertz (optimized for cuto tow defect)

Figure 9. Geometry of finite element model for internal flaw (cut tow).

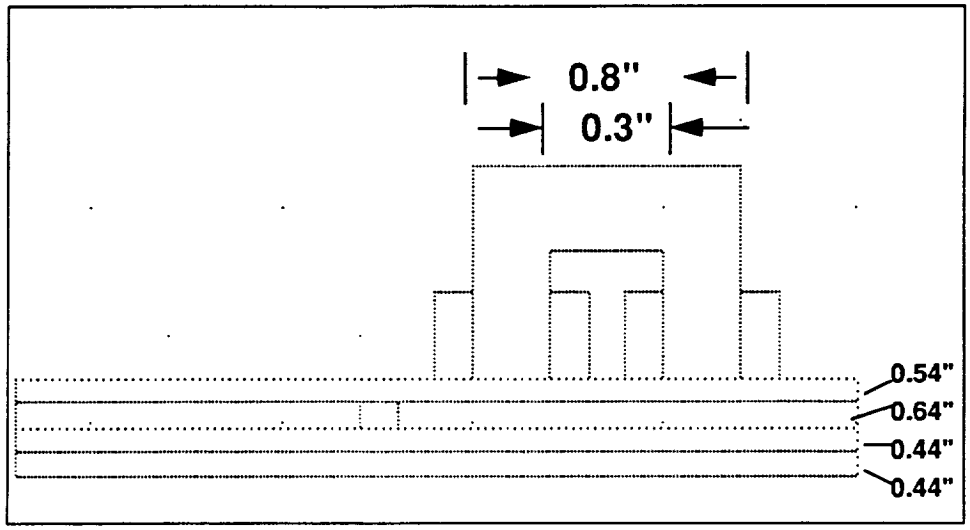


Figure 10. Finite element model showing magnetic field lines during eddy current scan when probe is away from the flaw.

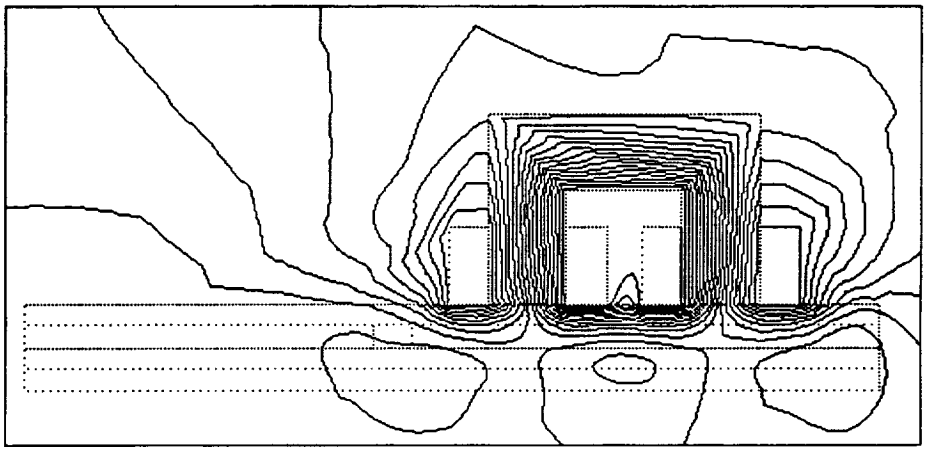

Figure 11. Magnetic flux lines when probe is over part.

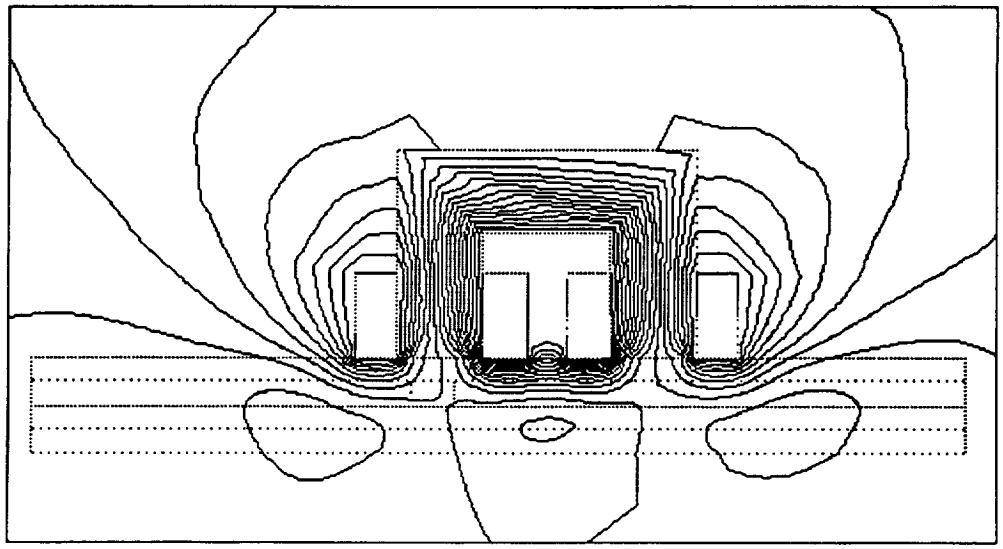

The Ansoft software provides the capability to generate a macro which allows one to simulate a scanning motion across the part being inspected. During each step across the part one can embed into the macro particular calcuations such as total impedance at the coil, J or M values along a line or within a region. For example in simulating the above scan, the information normally observed is the impedance response of the probe. By including a macro to increment in the x direction 0.05 inches each step within the mesh generating program and then including within the eddy current solver program the calculation for the $X_R$ and $X_L$ one obtains the following charts:

Figure 12(a). Chart showing expected eddy current resistance measurement when scanning part shown in Figures 10-11.

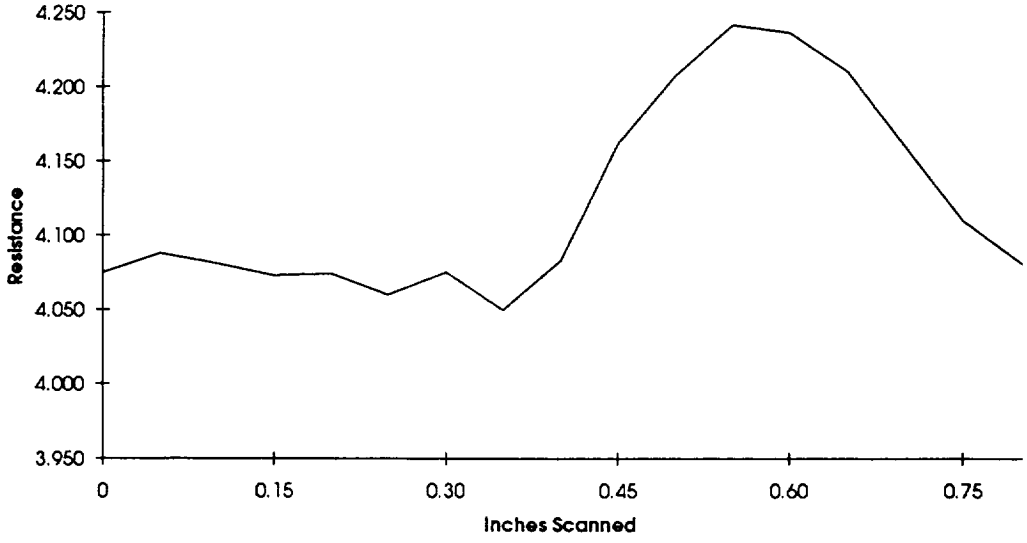

Figure 12(b). Chart showing expected eddy current reactance measurement when scanning part shown in Figures 11-12

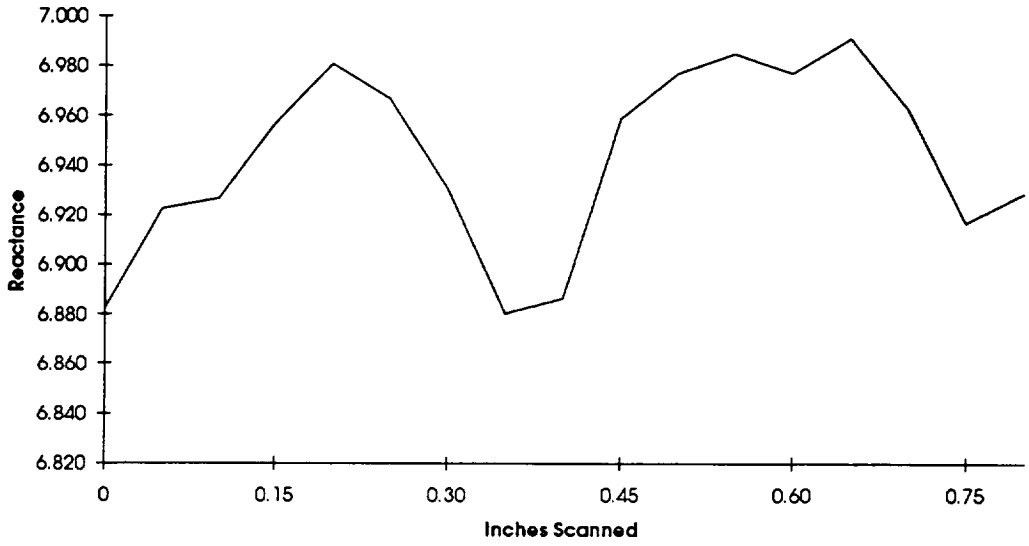


This simulated response can be compared with actual data obtained from an eddy current inspection.The experimental data obtained from the robotic eddy current workcell provides a much noiser signal. The following waveforms are obtained from scanning the thin filament wound case over regions of no known defects and regions with known defects.

Figure 13(a). Time varying reactance signals at 3.2 mhz for portion of sample with no defects.

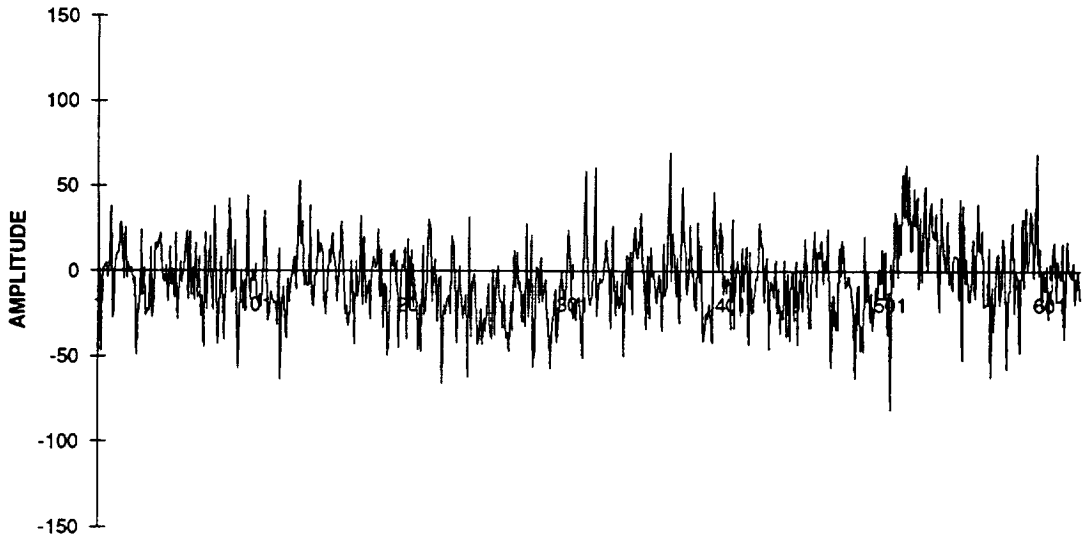

Figure 13(b). Frequency Spectrum

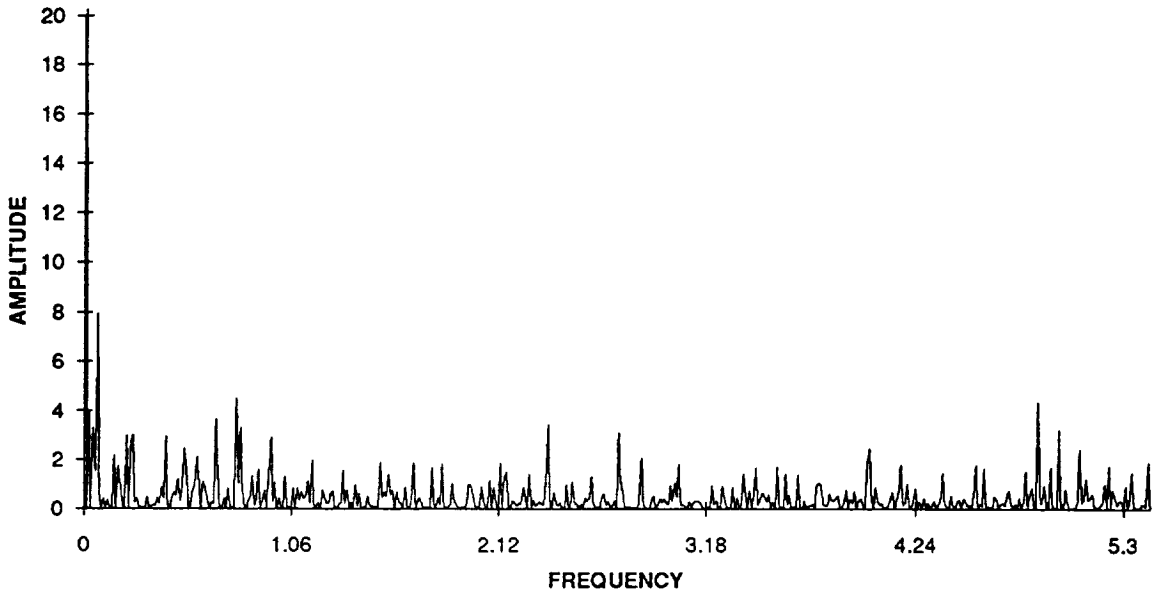


Figure 14(a). Time varying reactance data for region above cut tows.

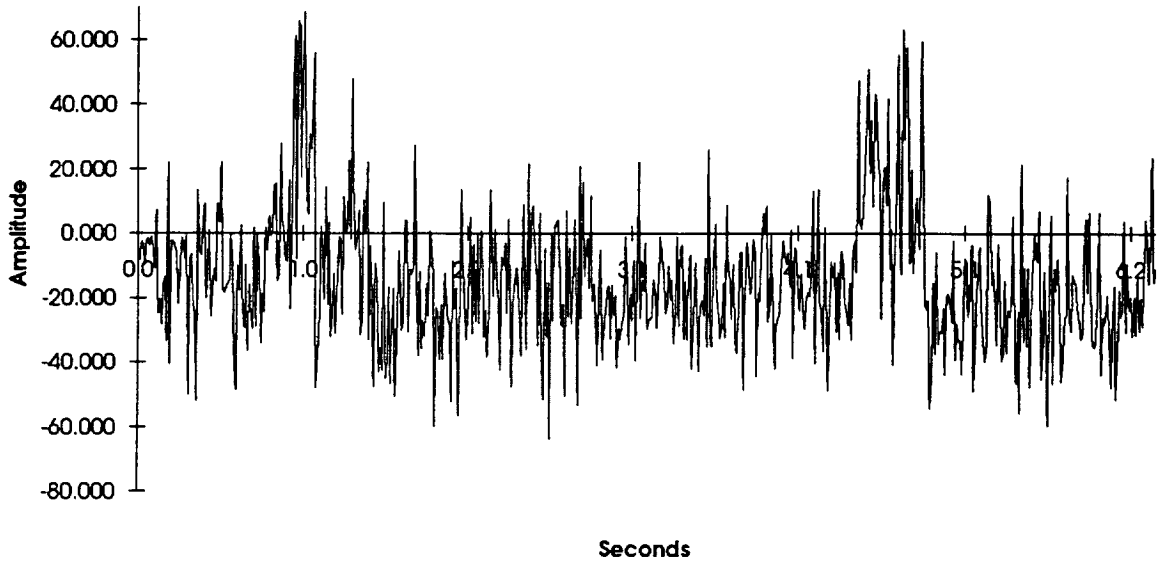


Figure 14 (b) Frequency Spectrum of the cut-tow region

Figure 14 (b) Frequency Spectrum of the cut-tow region

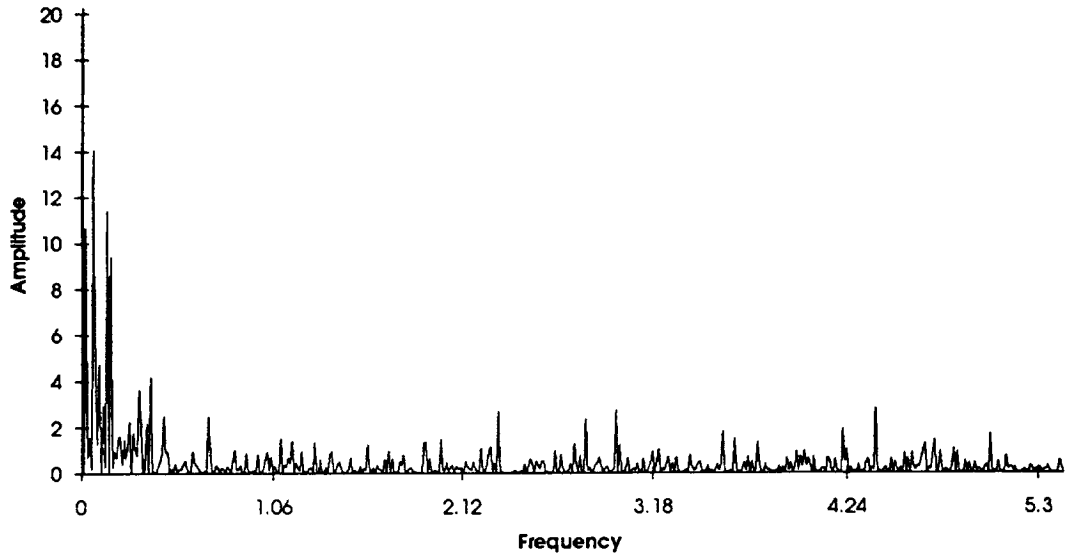


The relationship between time-varying components associated with the probe passing over the filaments was anticipated to very straigh-forward and easy to determine merely by matching large amplitude frequency components between the various defect regions and the region with no known defects. This methodology would have developed along the lines used by Doctor, et al;[34] except for the real time feature extraction required for the experts system approach. Unfortunately that did not work out too well. A lot of time was spect in trying to match up frequency components between the various spectra, performing an inverse FFT to obtain a noise free time based signal. In this trial and error approach only very small repetitive waveforms were removed. The large amplitude signals, which make the eddy current signal interpretation difficult, have persisted. Therefore it is still difficult to develop a set of rules which will enable an expert system to perform eddy current interpretation of graphite epoxy filament wound components.

Another useful concept which the modelling software allows, is to determine optimal geometries for the various probes. For example, a series of simulations illustrating how geometry affects the conductance measurement of the graphite epoxy filament material using the horseshoe probe are given next.

Figure 15(a). Finite element model showing longer coil on legs of the horseshoe.

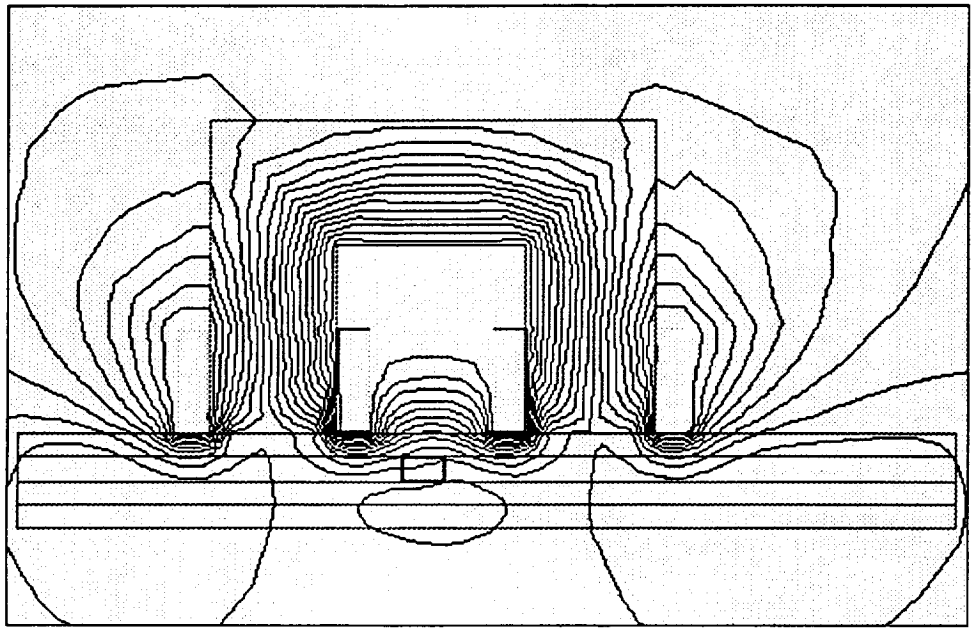

Figure 15(b). Finite element model showing larger horseshoe(approx. 1.5 times).

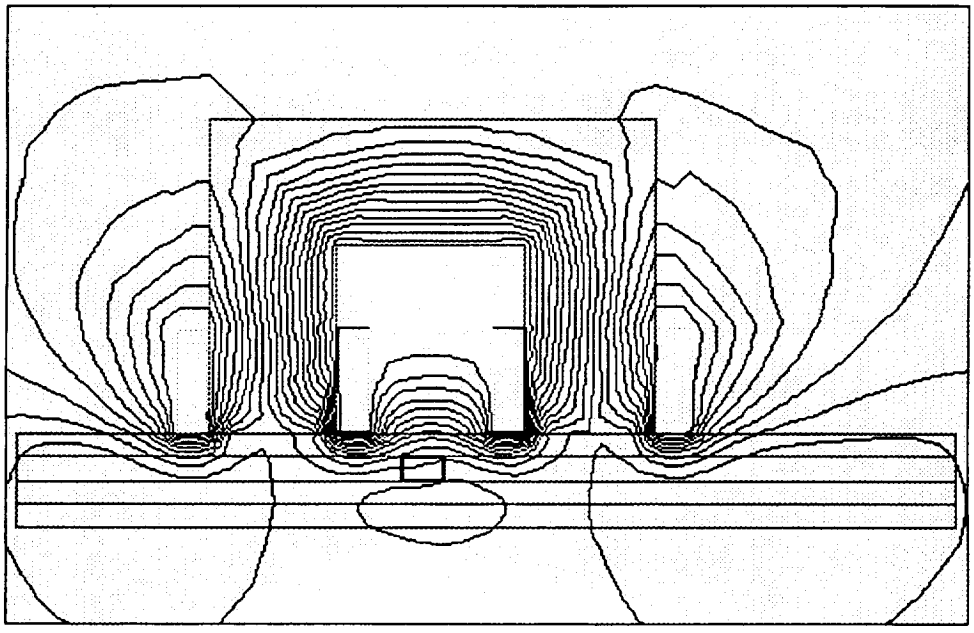

For the cases tried with the same defect geometry, the impedance measurements obtained are given in the following table:

| Case | Frequency | $R_{max}$ (ohms) | $R_{min}$(ohms) | $X_{max}$(ohms) | $X_{min}$(ohms) |
|---|---|---|---|---|---|
| 1. Normal | 3.2 Mhz | 4.242 | 4.075 | 6.991 | 6.882 |
| 2. longer coil | 3.2 Mhz | 4.068 | 3.982 | 7.52 | 7.61 |
| 3. larger probe | 3.2 Mhz | 3.379 | 3.562 | 7.29 | 7.50 |
| 4. larger probe | 1.0 Mhz | 1.499 | 1.529 | 3.15 | 3.32 |

The case identified as Normal is taken from the data shown in Figures 12(a) and (b). Note that with the same defect size in layer 2, the following changes in impedance are calculated:

| Case | $\Delta R$ | $\Delta X$ |
|---|---|---|
| 1 | 0.167 | 0.109 |
| 2 | 0.0086 | -0.09 |
| 3 | -0.183 | -0.21 |
| 4 | -0.0030 | -0.17 |

From this data, it is obvious that for the same defect modeled here, the largest signals for defect identification are obtained from the probe with the larger footprint. Case 4 was then run to see if a larger probe might respond better to a lower frequency; however, at the lower frequency, the magnetic flux density is too low to provide a good signal for the flaw. Hence, for graphite epoxy materials, larger probe sizes should provide larger signals for flaw detection.

## CONCLUSIONS

This research has continued to make in-roads into establishing theoretical foundations for the robotic eddy current inspection system in Building 4702 at Marshall Space Flight Center. The largest contributor to understanding how eddy current signals show respond to known types of defects is still the finite element software. In these studies, the finite element software used was "Maxwell", which is a product of Ansoft, Inc.

There is still some difficulty in scanning filament wound materials due to the surface roughness of the fabricated parts used in this study. An attempt was made to use FFT analysis to pick out signals from these surface effects; however, we were not successful in actually performing a good signal clean-up using FFT's as a post-processing tool. A better approach for experiments such as these is to consider using the new Digital Signal Processing units being offered in today's marketplace. The goal to develop a stand alone expert system for defect analysis will require such technology. Considerations of neural nets for cleaning up the noisy signals may also be considered.

ACKNOWLEDGEMENTS

We appreciate the assistance of the Mary Beth Cook and the other personnel in M & P Laboratory at Marshall Space Flight Center who provided samples and materials when needed. We also want to thank Mr. Ken Woodis for allowing to work in the NDE Laboratory.

REFERENCES

1. Vernon, S.N., "Probe properties Affecting the Eddy Current NDI of Graphite Epoxy", Review of Progress in Quantitative NDE, 7(1987), pp. 1113-1123.

2. Vernon, S.N., "Eddy Current Inspection of Thick Carbon Fiber Reinforced Composites", Review of Progress in Quantitative NDE, 8(1988), pp. 1543-1550.

3. Vernon, S.N., "Coupling Coefficient: A Determinant of Eddy Current Probe Performance", Review of Progress in Quantitative NDE, 9(1989).

4. Vernon, S.N., "The Universal Impedance Diagram of the Ferrite Pot Core eddy Current Transducer", IEEE Transactions on Magnetics, 25(1986), pp. 2639-2645.

5. Vernon, S.N., "Parametric Eddy Current Defect Depth Model and its Application to Graphite Epoxy", NDT International, 22(1989), pp. 139-148.

6. Vernon, S.N., "A Single-side eddy Current Method to Measure Electrical Resistivity", Materials Evaluation, 46(1988), pp. 1581-1587.

7. Vernon, S.N., P.M. Gammell, "Eddy Current Inspection of Broken Fiber Flaws in Non-metallic Fiber Composites", Review of Progress in Quantitative NDE,4(1985), pp. 1229-1237.

8. Sabbagh, H.A., S.N. Vernon, "Description and Verification of a Model of Eddy Current Probes with Ferrite Cores", Review of Progress in Quantitative NDE, 3A(1984), pp. 653-662.

9. Shull, P.J., T. EE. Capobianca, and J.C. Moulder, "Design and Characterization of Uniform Field Eddy Current Probes", Review of Progress in Quantitative NDE, 6A(1986), pp. 695-703.

10. Smith, E. "Uniform Interrogating Field Eddy Current Technique and its Applications", Review of Progress in Quantitative NDE, 5A(1985), pp. 165-176.

11. Cecco, V.S., G. Van Drunen, and F.L. Sharp, Eddy Current Manual, Vol. 1, Chalk River laboratories, Chalk River, Ontario.

12. Dodd, C.V., W.E. Deeds, "Absolute Eddy Current Measurements of Electrical Conductivity", Review of Progress in Quantitative NDE, 2(1982), pp.387-393.

13. Dodd, C.V., W.E. Deeds, "Analytical Solutions to Eddy Current Probe Coil Problems", Journal of Applied Physics, 39(1968), pp.2829-2838.

14. Ida, N., R. Palanisamy, and W. Lord, "Eddy Current Probe Design using Finite Element Analysis", Materials Evaluation, 41(1983), pp. 1389-1394.

15. Ida, N., "Three Dimensional Finite Element Modeling", Review of Progress in Quantitative NDE, 7(1987), pp.201-209.

16. Hower, G.L., "Stationary Formulas for Computing the Response in Eddy Current NDE", Journal of Nondestructive Evaluation. Vol. 6, No. 4, 1987.

17. Auld, B.A., F.G.Muennemann, and M. Riazent, "Quantitative Modeling of Flaw Response in Eddy Current Testing", chapter 2, Nondestructive Testing, Vol. 7, Academic Press. London, 1984.

18. Zaman, J.M., C.G. Garadner, and S.A. Long, "Change in Impedance of a Single-Turn Coil Due to A Flaw in A Conducting Half Space", Journal of NDE, Vol. 3, No. 1, 1982.

19. Auld B.A., F. Muennemann, and D.K. Winslow, "Eddy Current Probe Response to Open and Closed Surface Flaws", Journal of NDE, Vol. 2, pp. 1-21, 1981.

20. Bowler, J.R., H.A. Sabbagh and L.D. Sabbagh, " Eddy Current Probe Impedance due to Interaction with Advanced Composites", Review of Progress in Quantitative NDE, 7(1987), pp.1021-1027.

21. Beissner R.E., "A Multilayer Eddy Current Model for Advanced Composites", Review of Progress in Quantitative NDE, 10A(1990).

22. Bowler, J.R., J. of Applied Physics, 61, 833(1987).

23. Doctor, P.G., "Pattern Recognition in Methods for Characterizing and Sizing Flaws using Eddy Current Data", Eddy Current Characterization of materials and Structures, ASTM STP 722, (1981), pp 461-483.

24. Upda, L. and S.S. Upda, "Eddy Current Defect Characterization Using Neural Networks", Materials Evaluation, 48(1990), pp 342-347.

25. Upda, L. and W. Lord, "A Search-based Imaging System for Electromagnetic Nondestructive Testing", IEEE Expert 4, (1989) 18-26.

26. Upda, L. and W. Lord, "An AI Approach to Eddy Current Defect Characterization problem", Review of Progress in Quantitative NDE, 8(1988), pp 899-906.

27. Palanisamy, R., "Developments in Eddy Current Nondestructive Testing", Materials Evaluation, 49(1991), pp. 1158-1161.

28. Hower, G.L., "Stationary Formulas for Computing the Response in Eddy Current NDE", Journal of Nondestructive Evaluation. Vol. 6, No. 4, 1987.

29. Auld, B.A., F.G.Muennemann, and M. Riazent, "Quantitative Modeling of Flaw Response in Eddy Current Testing", chapter 2, Nondestructive Testing, Vol. 7, Academic Press. London, 1984.

30. Zaman, J.M., C.G. Garadner, and S.A. Long, "Change in Impedance of a Single-Turn Coil Due to A Flaw in A Conducting Half Space", Journal of NDE, Vol. 3, No. 1, 1982.

31. Bahr, A., "Microwave Eddy Current Techniques for Quantitative Nondestructive Evaluation", Eddy Current characterization of Materials and Structures, ASTM, Philadelphia, 1981, pp.311-331.

32. Auld B.A., F. Muennemann, and D.K. Winslow, "Eddy Current Probe Response to Open and Closed Surface Flaws", Journal of NDE, Vol. 2, pp. 1-21, 1981.

33. Beissner R.E., "A Multilayer Eddy Current Model for Advanced Composites", Review of Progress in Quantitative NDE, 10A(1990).

34. Doctor, P.G., "Pattern Recognition in Methods for Characterizing and Sizing Flaws using Eddy Current Data", Eddy Current Characterization of materials and Structures, ASTM STP 722, (1981), pp 461-483.

35. Upda, L. and S.S. Upda, "Eddy Current Defect Characterization Using Neural Networks", Materials Evaluation, 48(1990), pp 342-347.

36. Upda, L. and W. Lord, "A Search-based Imaging System for Electromagnetic Nondestructive Testing", IEEE Expert 4, (1989) 18-26.

APPENDIX

The following program is used to calculate a 3D response from the E field data obtained from Ansoft Maxwell models.

Program RECIPRO.C

```
# include <stdio.h>
# include <math.h>
# include <string.h>
# include <dos.h>

float y[200];
float ans1;
float ansv;
int xxl1;
int xxh1;
int i1;
int numseg;
float sp;
float i;
```

```
void IntegrateVector(float y[],float samper,int xl,int
xh,float *ans);

void ClrScr();

void main()
{
   int j = 0;
   float ef[200];
   float df[200];
   float cond;
   float cur;
   float delx;
   float dely;
   float delz;
   char ext[] = ".dat";
   char dfield[200];
   char efield[200];
   char dname[20];
   char ename[20];
   FILE *dstream;
   FILE *estream;

   ClrScr();        /*clear screen*/

   printf("  Please enter 'E-field without flaw' file name
: ");
   gets(ename);
   strcat(ename,ext);
   printf("  Please enter 'E-field with flaw' file name :
");
   gets(dname);
   printf("  Please enter 'conductivity' of specimen : ");
   scanf("%e", &cond);
   printf("  Please enter 'source current' : ");
   scanf("%f", &cur);
   printf("  Please enter 'defect depth' : ");
   scanf("%f", &dely);
   printf("  Please enter 'defect width' : ");
   scanf("%f", &delx);
   printf("  Please enter 'defect length': ");
   scanf("%f", &delz);
   strcat(dname,ext);

   estream = fopen(ename, "r");
   dstream = fopen(dname, "r");


   /*read file*/
   while(fgets(efield, 64, estream) && fgets(dfield, 64,
dstream)!=NULL)
   {
     ef[j] = atof(efield+44);
     df[j] = atof(dfield+44);
```

```
      y[j] = fabs(ef[j] * df[j])/(cond*cur*cur);
      j = j + 1;
    }

    /* calculate the impedance change */
    xxl1 = 0.0;
    xxh1 = 99.0;
    sp = dely / 100.0;
    IntegrateVector(y, sp, 0.0, 99.0, &ans1);
    ansv = ans1 * delx * delz;
    printf("The Impedance Change = %e\n", ansv);
}


/* 1/3 and 3/8 Simpson rule */
void IntegrateVector(float y[],float samper,int xl,int
xh,float *ans)
{
    int numseg;
    int i;
    int strtpnt;
    int endpnt;
    int segcntr;
    float area1;
    float area2;
    float area;
    char even;
    float segwidth;

    numseg = xh - xl;
    segwidth = samper;
    endpnt = xh;
    area1 = 0.0;
    area2 = 0.0;
    area = 0.0;

    if ( fmod(numseg,2) != 0 )
   {
        area1 = 3.0 / 8.0 * segwidth * (y[endpnt - 3] + 3.0 *
                y[endpnt - 2] + 3.0 * y[endpnt - 1] +
y[endpnt]);
        endpnt = endpnt - 3;
   }

    else
   {
        area1 = 0.0;
   }

    if ( numseg != 3 )
   {
        strtpnt = xl;

        do
```